Seasonal responses of $\delta^{13}C$ and $\delta^{18}O$ of atmospheric CO_2 over sub-urban region of India

Mahesh Pathakoti[1*], A.L. Kanchana[1], D.V. Mahalakshmi[1], Sreenivas G[2], Tania Guha[3,4], Vijay Kumar Sagar[1], P.Raja[5],and SeshaSai M.V.R[1]

[1]Earth and Climate Sciences Area (ECSA), National Remote Sensing Centre (NRSC), Indian Space Research Organisation (ISRO), Hyderabad-500037, India.

[2]Department of Physics, Jawaharlal Nehru Technological University, Hyderabad, 500085, India

[3]Department of Geography, University of Calgary, Calgary, Alberta, Canada

[4]Previously at Indian Institute of Tropical Meteorology, Pune, India

[5]ICAR-Indian Institute of Soil and Water Conservation, Research Centre,Ooty, The Nilgiris, Tamil Nadu, - 643004,India.

*Corresponding author: Mahesh Pathakoti (mahi952@gmail.com)

Key Points:

- The Study focused on diurnal variability of seasonal averaged atmospheric CO_2 concentration and its stable isotopes ($\delta^{13}C$-CO_2 and $\delta^{18}O$-CO_2).
- Determination of $\delta^{13}C$ signature of atmospheric CO_2 using improved Miller and Tans model.
- The effect of the Indian summer monsoon circulation on atmospheric CO_2 variation was studied.

Abstract

Seasonal and diurnal variability of atmospheric CO_2 and its driving factors are studied using its continuous monitoring of concentration and isotopic ratios ($\delta^{13}C$-CO_2 and $\delta^{18}O$-CO_2) for the first time over Shadnagar, a sub-urban location of India with high precision *in-situ* data from November 2018 to October 2019. The annual averaged atmospheric CO_2 concentrations, $\delta^{13}C$-CO_2 and $\delta^{18}O$-CO_2 are 414.76±4.26 ppm, -11.19±1.63 ‰ and 9.02 ±12.78 ‰. Maximum seasonal diurnal variability of atmospheric CO_2 was observed in summer monsoon (17.30 ± 9.29 ppm) and the minimum was noticed in winter (7.19 ± 0.11 ppm) indicating strong seasonality at the study site. To characterize the atmospheric CO_2 sources, an improved model of Miller and Tans was implemented by plotting ΔCO_2 against $\Delta(CO_2 \times \delta^{13}C)$ respectively during day and night. However, a strong source/sink signature of $\delta^{13}C$ was observed during nighttime of summer monsoon with a slope of -37.42 ± 0.73 ‰, obtained using a reduced major axis (RMA)

regression.The source identified is attributed to combustion and dominance of C_3 ecosystem respiration respectively. The seasonal relationship between $\delta^{18}O$-CO_2 and $\delta^{13}C$-CO_2 is strongly correlated during pre-monsoon ('r' = 0.93-0.95) than post-monsoon ('r' = 0.07-0.13), which might be due to high vapour pressure deficit. A Lagrangian back-trajectory model confirms the influence of the Indian summer monsoon on the variability of atmospheric CO_2 concentration during the summer monsoon season.

Keywords: atmospheric CO_2, reduced major axis,Miller and Tans, Indian summer monsoon.

1. Introduction

The Intergovernmental Panel for Climate Change (IPCC) reported that carbon dioxide (CO_2) sources from anthropogenic gases in the atmosphere cause more radiative forcing next to water vapor (Smith et al., 1999). CO_2 concentrations are consistently increasing and touched 400 ppm at Mauna Loa, a global reference site during May 2013 (Monastersky, 2013). Globally, CO_2 concentrations are increasing, which could be due to land use land cover changes (LULCC) and progress in industrial activities (Ballantyne et al., 2012) especially fossil fuel combustion, cement manufacturing etc.. Due to fossil fuels burnings and LULC emissions, an increase of 40 and 150 % in CO_2 and CH_4 concentration respectively is observed since the pre-industrial period (Huang et al., 2015). Emissions of CO_2 by different processes are controlled by varied environmental conditions, in which about half of the CO_2 levels are released into the atmosphere as source and remaining are absorbed by the processes of the terrestrial biosphere and ocean uptake (Andres et al., 1996) as sink. Hence monitoring and maintaining long-term records of atmospheric CO_2 measurements are very important to understand the carbon cycle and to assess the CO_2 mixing ratios in the atmosphere by controlling factors namely photosynthesis, respiration, biomass, fossil fuel burning and air-sea exchange processes (Machida et al., 2003).

Globally, systematic high precision atmospheric CO_2 observations are accelerated to understand the global carbon cycle. Over the Indian subcontinent, spatio-temporal variability in atmospheric CO_2 concentrations are characterized by the terrestrial biosphere and seasonal weather patterns which brings long-range air-masses (Valsala et al., 2013; Tiwari et al., 2014). To understand the seasonal, inter and intra annual variations of atmospheric CO_2 over the Indian subcontinent, high precision CO_2 measurements are being generated across the country from different research institutes (Bhattacharya et al., 2009; Sharma et al., 2014; Mahesh et al., 2016; Nalini et al., 2019). A literature survey on atmospheric CO_2 variability over the Indian region is mainly focused on local sources and transport (Sreenivas et al., 2016). However, a need was felt to understand the reasons and causes for uncertainty in surface fluxes. Hence an advanced studies of stable isotopic measurements of carbon and oxygen are gaining momentum to understand CO_2 levels, source and sinks of CO_2, both on regional and global levels.

Stable carbon and oxygen isotopes of atmospheric CO_2 can be used as tracers in the carbon cycle, which are affected by the anthropogenic and biogenic CO_2 components. The $\delta^{13}C$-CO_2 and $\delta^{18}O$-CO_2 are stable isotopes of CO_2 molecules are widely used for source apportionments in the atmosphere, hydrosphere and geosphere as well as interaction between them (Guillon et al., 2015). The $\delta^{13}C$-CO_2 concentration in the atmosphere has been decreasing since pre-industrial times, which indicates the more addition of CO_2 to the atmosphere by fossil fuel burning (Yakri, 2011). Many research activities have been carried on atmospheric CO_2 and its stable isotopes ($\delta^{13}C$-CO_2 and $\delta^{18}O$-CO_2) by various groups (Bhattacharya et al., 2009; Pataki et al., 2003;

Clark-Thorne and yapp, 2003; Francey and Tans, 1987; Murayama et al., 2010; Newman et al, 2003; Wada et al., 2003; Pataki et al., 2006; Zhou et al., 2005; Zhou et al., 2006; Sturm et al., 2006; Djuricin et al., 2010; Guha and Ghosh, 2010, 2013, 2015; Gorka and Lewicka- Szczebak, 2013; Liu et al., 2014; Pang et al., 2016). Liu et al. (2014) studied the atmospheric CO_2, $\delta^{13}C$-CO_2 composition and their relationship to understand the sources and sinks at two stations viz., Waliguan and Shangdianzi in China using observational data for the period from 2007 to 2010. The result of this study indicates that CO_2 and $\delta^{13}C$-CO_2 composition possesses long-term trends and seasonal cycles that correlate with each other. An improved model by Miller and Tans (2003) is widely used to determine the source or sink that causes CO_2 variability. Pang et al. (2016) used Keeling plot intercept method for isotopic composition of CO_2 and found increased value in vegetative season and depleted value in heating season. A few studies were carried on atmospheric CO_2 and its stable isotopes in India, which are limited to discrete sample analysis (Bhattacharya et al., 2009; Guha and Ghosh, 2013, 2015). The present study on atmospheric CO_2 and its stable isotopes was carried using laser based Isotope ratio Infrared spectrometer analyser. Measurements of the $\delta^{18}O$-CO_2 also play an important role in the carbon cycle to distinguish the photosynthesis and respiration process of CO_2 fluxes (Farquhar et al., 1993; Kato et al., 2004).

The objective of the present study is to understand diurnal variability of seasonal atmospheric CO_2 and its stable isotopic composition at the sub-urban region, of Telangana, India. Since the study site is surrounded by multiple sources for CO_2 (*e.g.,* biospheric respiration and fossil fuel emissions), thus an improved model by Miller and Tans (2003) was used to characterize the CO_2 sources/sinks. Here, we report continuous high precision CO_2 isotopic measurements, first of their kind from sub-urban region, of Telangana. This work has been carried out as part of the Atmospheric CO_2 Retrieval and Monitoring (ACRM) of the National Carbon Project (NCP) funded by the Climate and Atmospheric Processes of ISRO-Geosphere Biosphere Programme (CAP-IGBP).

2. Materials and Methods

Observations of CO_2 and its isotopic composition are measured during November 2018 to October 2019 by laser based Isotope Ratio Infrared Spectrometer (IRIS) analyser. This instrument is installed at 8 m height from the surface of ASL, NRSC, Shadnagar (Latitude: 17.09 °N; Longitude: 78.21 °E and Elevation: 648 m above mean sea level), a sub-urban region, northern side of Hyderabad(~ 60 km away). Thus our study site is near to the highly populated city of Hyderabad.

Surface meteorological data at the study site are collected from an automatic weather station. An hourly Boundary Layer Height (BLH) were obtained from European Centre for MediumRange Weather Forecasts (ECMWF-ERA, https://cds.climate.copernicus.eu/cdsapp#!/dataset/reanalysis-era5-single-levels?tab=form). In addition to the above datasets, fire counts with confidence interval of > 70% are considered from Moderate Resolution Imaging Spectroradiometer(MODIS). Normalized Difference vegetation Index (NDVI) is obtained from an open data archival of Bhuvan site (https://bhuvan-app3.nrsc.gov.in/data/download/index.php), which is derived from Oceansat-2 Ocean color monitor sensor. Figure 1 shows that the study area is overlaid with NDVI as well as time series of air temperature, relative humidity and wind speed recorded at the study site.

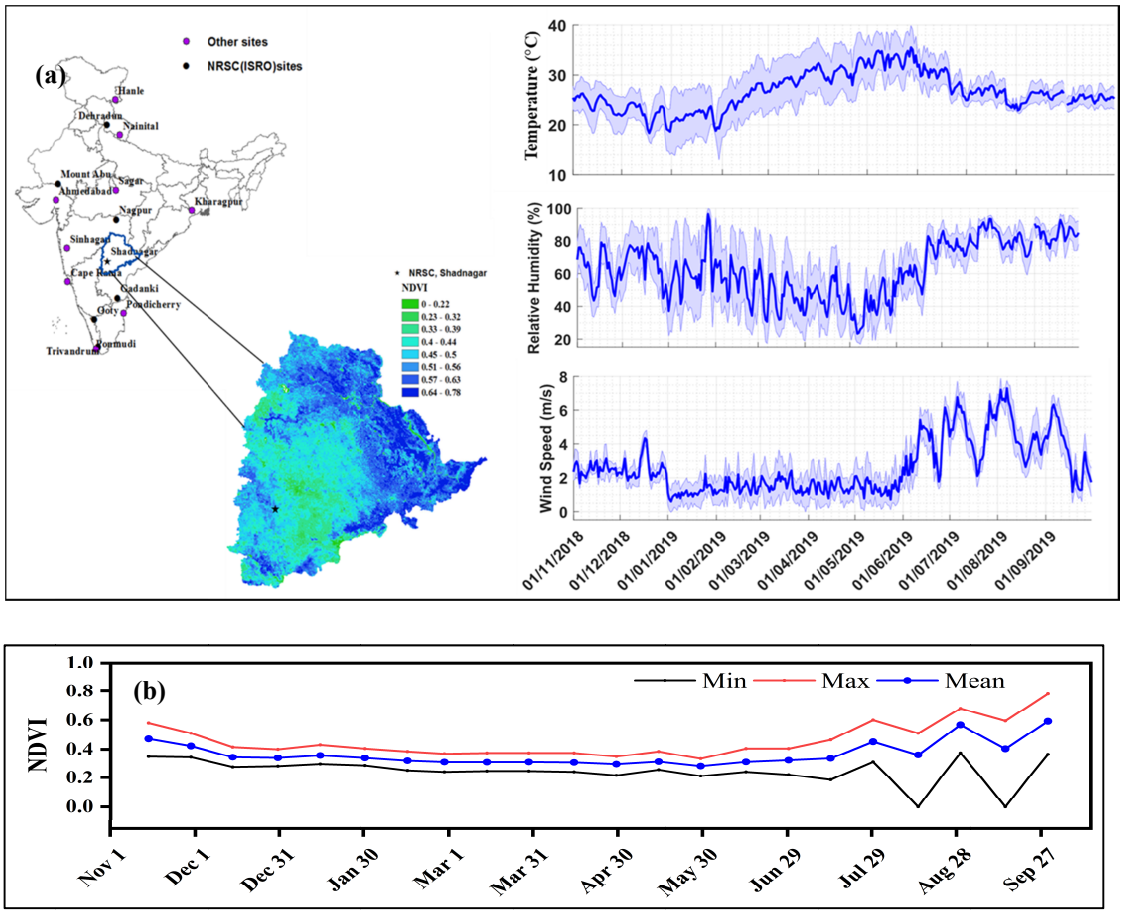

Figure 1. (a) Study location with prevailing weather conditions and (b) NDVI

Figure 1 also shows *in-situ* atmospheric CO_2 networks across the country established by different research institutes of India. A few of the station's information is obtained from Nalini et al. (2019). Black solid circles are the atmospheric CO_2 measurement stations installed under ACRM of NCP project by NRSC, ISRO. At the present study site (solid black star) long-term CO_2, CH_4 and H_2O measurements are complemented by CO_2 and N_2O isotopic observations. During the study period, air temperature is observed to be high in pre-monsoon (March-May) with maximum air temperature of 43°C and low in winter (January-February) with mininum temperature of 9°C. Relative humidity is observed to be high in monsoon (June-September) with maximum value reaching 100% and low in pre-monsoon with minimum of 12.18%. However, wind speed is observed to be ranging from 0.005 m s^{-1} to 6.0 m s^{-1} during the study period. Seasonal NDVI during the study period for post-monsoon, winter, pre-monsoon and monsoon are 0.39, 0.33, 0.30 and 0.41 respectively.The study site is about 60 km away from the urban region of Hyderabad (fifth largest city in India) associated with 75% air pollution from traffic sector alone (significant anthropogenic impacts) due to increase in population and related factors

(Mahalakshmi et al., 2014).Thus the present study site doesn't fall under single source contributor of atmospheric CO_2.

2.1. Continuous stable isotopic measurements

In this study, we used commercial laser based IRIS CO_2 Carbon Isotope analyzer Enhanced Performance (CO_2-CCIA-EP), procured from Los Gatos Research, U.S.A in November 2018. Details of the instrument functioning are given in Baer et al. (2002). The CO_2-CCIA-EP is capable of simultaneous measurements of dry CO_2, ^{13}C, ^{18}O and H_2O are measured using the absorption line at 2.05 μm with 1 Hz frequency and uses a performance enhancing off-axis cavity ring down spectroscopy. Mole fraction of isotopic composition also depends on internal cavity pressure and temperature hence maintained constant at 119.14 Torr and 45.36 °C respectively (Mahesh et al., 2015). To keep the moisture as constant and as low as possible in the analyzer, sample and reference gases are passed through a Neflon drying unit. The dry-air mole fractions of CO_2 where the measured mole fraction of H_2O, which is also in ppm has been removed as shown in Equation 1.

$$CO_2(\text{ppm})_{\text{dry}} = \left(\frac{CO_2\ (\text{ppm})_{\text{wet}}}{(1 - \frac{H_2O\ (\text{ppm})}{10^6})} \right) \quad (1)$$

The ^{13}C-CO_2 and ^{18}O-CO_2 compositions are reported as $\delta^{13}C$ and $\delta^{18}O$ respectively versus VPDB (Vienna Pee Dee Belemnite) and reported in per mil (‰) as shown in Equation (2) and (3)

$$\delta^{13}C\ (‰) = \left(\frac{C_s}{C_r} - 1\right) \times 1000 \quad (2)$$

$$\delta^{18}O\ (‰) = \left(\frac{O_s}{O_r} - 1\right) \times 1000 \quad (3)$$

Where C_s, C_r, O_s, and $O_r$defined as follows; $C_{s\ (sample)} = (^{13}C/^{12}C)_s$; $C_{r\ (VPDB)} = (^{13}C/^{12}C)_r$; $O_{s\ (sample)}=(^{18}O/^{16}O)_s$ and $O_{r\ (VPDB)} =(^{18}O/^{16}O)_r$

2.2. Calibration of CO_2 isotope analyzer

The CO_2-CCIA-EP is calibrated using National Oceanic and Atmospheric Administration (NOAA) supplied CO_2 isotope calibration reference gases (ID: CC718409) towards reporting data, eliminating instrument drifts and generating high quality data during the period of study. The precision and accuracy of the instrument are computed by performing the internal calibration(4 times) at frequent intervals (24th February 2019, 11th June 2019, 6th August 2019 and 8th January 2020). The resultant calibration showed a variation of 404.38±0.14 ppm of CO_2, -8.63±0.04 ‰ VPDB of $\delta^{13}C$-CO_2 and -1.41±0.07 ‰ VPDB of $\delta^{18}O$-CO_2 respectively. An inflow of reference gas has been passed through the Neflon drying unit for 5 minutes and collected data at 1 Hz frequency.

The 100 sec (1 σ) average precision of CO_2, $\delta^{13}C$-CO_2 and $\delta^{18}O$-CO_2 are 0.20 ppm, 1.1 ‰ and 7.19 ‰ and their respective drift are 0.074 ppm, 0.085 ‰ and 0.485 ‰ respectively. The result of the calibration report is summarized in table 1.

Cylinder ID	$\frac{CO_2(\text{ppm, ref}) \pm 1\sigma}{CO_2\ (\text{ppm, M}) \pm 1\sigma}$	$\frac{\delta^{13}C \text{ of } CO_2\ (‰, \text{ref}) \pm 1\sigma}{\delta^{13}C \text{ of } CO_2\ (‰, \text{M}) \pm 1\sigma}$	$\frac{\delta^{18}O \text{ of } CO_2\ (‰, \text{ref}) \pm 1\sigma}{\delta^{18}O \text{ of } CO_2\ (‰, \text{M}) \pm 1\sigma}$
NOAA,CC718409	$\frac{404.53 \pm 0.21\ (\text{ppm})}{404.38 \pm 0.14\ (\text{ppm})^*}$	$\frac{-8.45 \pm 0.01\ (‰, \text{VPDB})}{-8.63 \pm 0.04\ (‰, \text{VPDB})^*}$	$\frac{-1.28 \pm 0.03\ (‰, \text{VPDB})}{-1.41 \pm 0.07\ (‰, \text{VPDB})^*}$
Bias (Ref-M)	0.15 (ppm)	0.18 (‰)	0.13 (‰)
Precision	0.07%	0.54%	5.4%
Accuracy	0.04%	3.20%	16.4 %
Ref: Reference; M: Measured		*Indicates means of 100sec of 5 min calibration for 4 times calibration	

Table 1 Calibration report of CO_2, $\delta^{13}C$-CO_2 and $\delta^{18}O$-CO_2.

Bias between reference and measured values of CO_2, $\delta^{13}C$-CO_2 and $\delta^{18}O$-CO_2 are 0.15 ppm, 0.18 ‰ and 0.13 ‰ respectively.The precision and accuracy of CO_2, $\delta^{13}C$-CO_2 and $\delta^{18}O$-CO_2 are deduced with an averaging time of 100 sec. Results of the calibration in precision term are 0.07 %, 0.54% and 5.4% for CO_2, $\delta^{13}C$-CO_2 and $\delta^{18}O$-CO_2 respectively. The precision of $\delta^{18}O$-CO_2 is coarse compared $\delta^{13}C$-CO_2, which may be improved by performing calibration for longer averaging time. However, one needs to be compromised for the precision averaging time (Guillon et al., 2015). The second level quality was applied to the raw data by adjusting the respective biases.

2.3. Isotopic fraction using Improved model by Miller and Tans

Present study implemented Thoning et al. (1989) to compute the curve fitting and smoothing of the recorded time series data. To account, the strong atmospheric mixing of CO_2 during daytime, active convective boundary layer, the entrainment of background air in the free troposphere to surface layer, the Miller and Tans et al. (2003) proposed an improved model to compute the biases (Δ) between the recorded and smoothed values. In the present study, the Thoning et al. (1989) curve fitting function consist of a 3 polynomial and 4 harmonics terms as described in equation 4, which approximates the long-term trend, short-term variations due to local influence and a non-sinusoidal annual cycle respectively (https://gml.noaa.gov/ccgg/mbl/crvfit/index.html, accessed on 20 July, 2021).

$$f(x) = a_0 + a_1 x + a_2 x^2 + a_3 \sin 2\pi x + a_4 \cos 2\pi x + a_5 \sin 4\pi x + a_6 \cos 4\pi x \quad (4)$$

here x is time stamp for the input data and f(x) is (CO_2 or $\delta^{13}C$) time dependent variable. The smoothed data, trend, detrended seasonal cycle, seasonal amplitude and growth rate are computed using the equation 4.

Subsequently, we computed biases (Δ) of CO_2, $\delta^{13}C$-CO_2 and $\delta^{18}O$-CO_2 respectively in order to calculate the isotopic signature as explained by Miller and Tans et al. (2003). Following equation is the improved model by Miller and Tans, which was implemented in the present study.

$$(\delta^{13}C \times CO_2)_{obs} - (\delta^{13}C \times CO_2)_{smooth} = \delta_s\left(CO_{2_{obs}} - CO_{2_{smooth}}\right) \quad (5)$$

δ_s, $CO_{2_{obs}}$ and $CO_{2_{smooth}}$ in equation 5 are slope representing multiple sources, observational CO_2 and smoothed CO_2 derived from the equation 4 respectively. A linear relationship between ΔCO_2 and $\Delta(\delta^{13}C \times CO_2)$ which is popularly known as Miller Tans plot (Miller and Tans, 2003), was further studied. This linear relation is fitted with a ordinary least square (OLS) regression and the slope of the regression line is the carbon isotopic ratio ($\delta^{13}C$) of source CO_2. The Miller Tans model was applied on both day (10:00 Indian Standard Time (IST) till 18:00 IST) and night time (22:00 IST till 06:00 IST) hours during the study period. The OLS is more commonly known as linear regression which may be simple regression or multiple depending on number of explanatory variables. Generic model of the OLS is defined as shown in Equation (6).

$$y = a_0 + \sum_{i=1}^{n} \delta_i x_i + \epsilon \quad (6)$$

where y is $\Delta(\delta^{13}C \times CO_2)$, the dependent variable, a_0 is the intercept of the model, δ_i and x_i are the slope and ΔCO_2 corresponds to the i^{th} explanatory variable of the model (i = 1 to n), and ϵ is the random error. Similarly, equations 5 and 6 are implemented for computing the slope between ΔCO_2 versus $\Delta(\delta^{18}O \times CO_2)$. Both the variable in the Miller Tans plot, ΔCO_2 and $\Delta(\delta^{13}C \times CO_2)$, is associated with a measurement error. Moreover, the OLS regression generally yields slopes with larger error (Miller and Tans, 2003), so reduced major axis regression (RMA) (Cantrell, 2008) was further used to estimate the slope. In RMA regression the error in both the variable was accounted while estimating the source value and the standard error obtained was reported. With these methods, further results are discussed in the following sections.

286
287
288
289
290

3.Results and Discussion

3.1. Seasonal and Diurnal variation of CO_2, $\delta^{13}C$-CO_2 and $\delta^{18}O$-CO_2

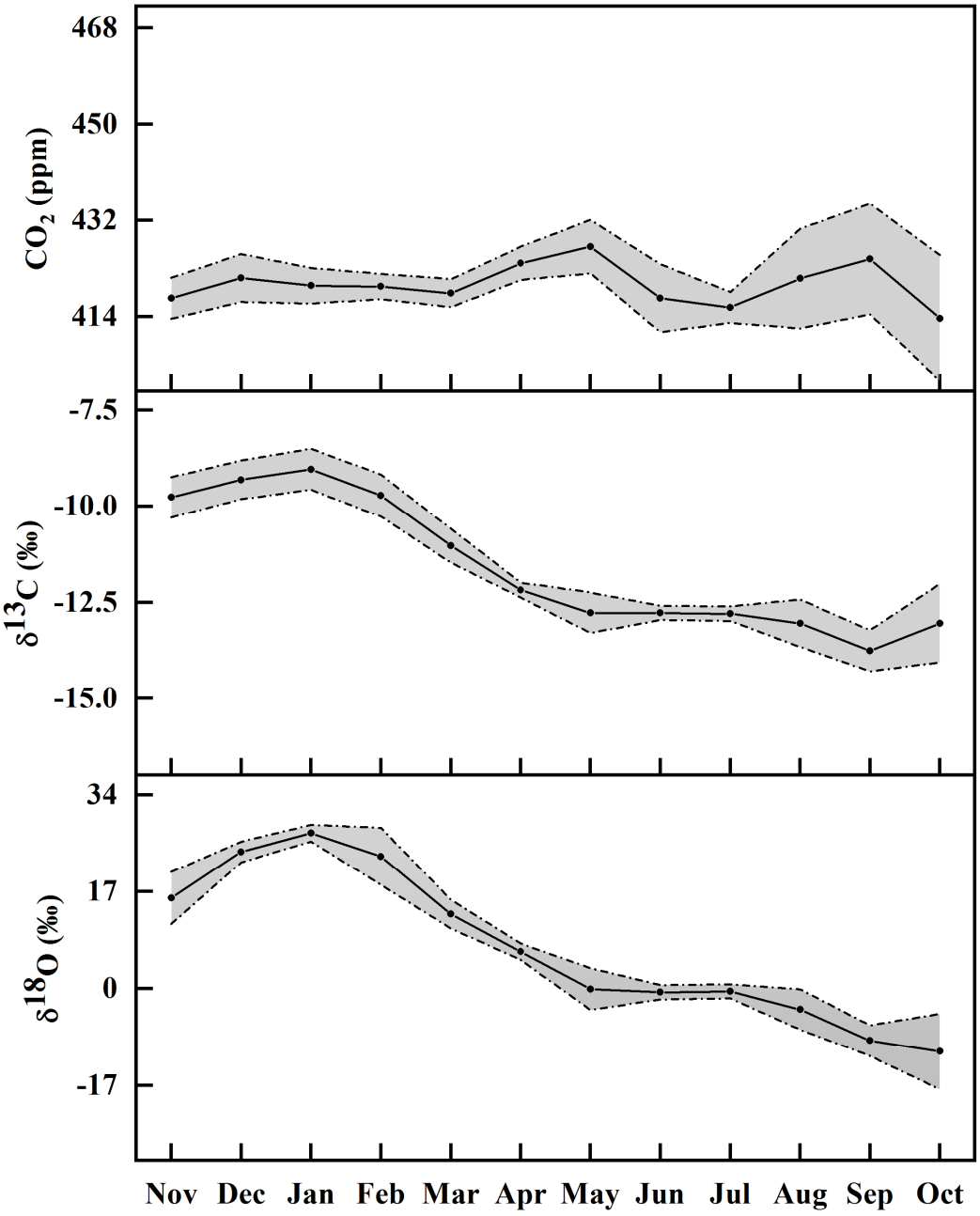

291
292
293
294

Figure 2. Seasonal variation of atmospheric CO_2 (top), $\delta^{13}C$-CO_2 (middle) and $\delta^{18}O$-CO_2 (bottom). Grey shaded region represents the 1 standard deviation (STD).

295
296

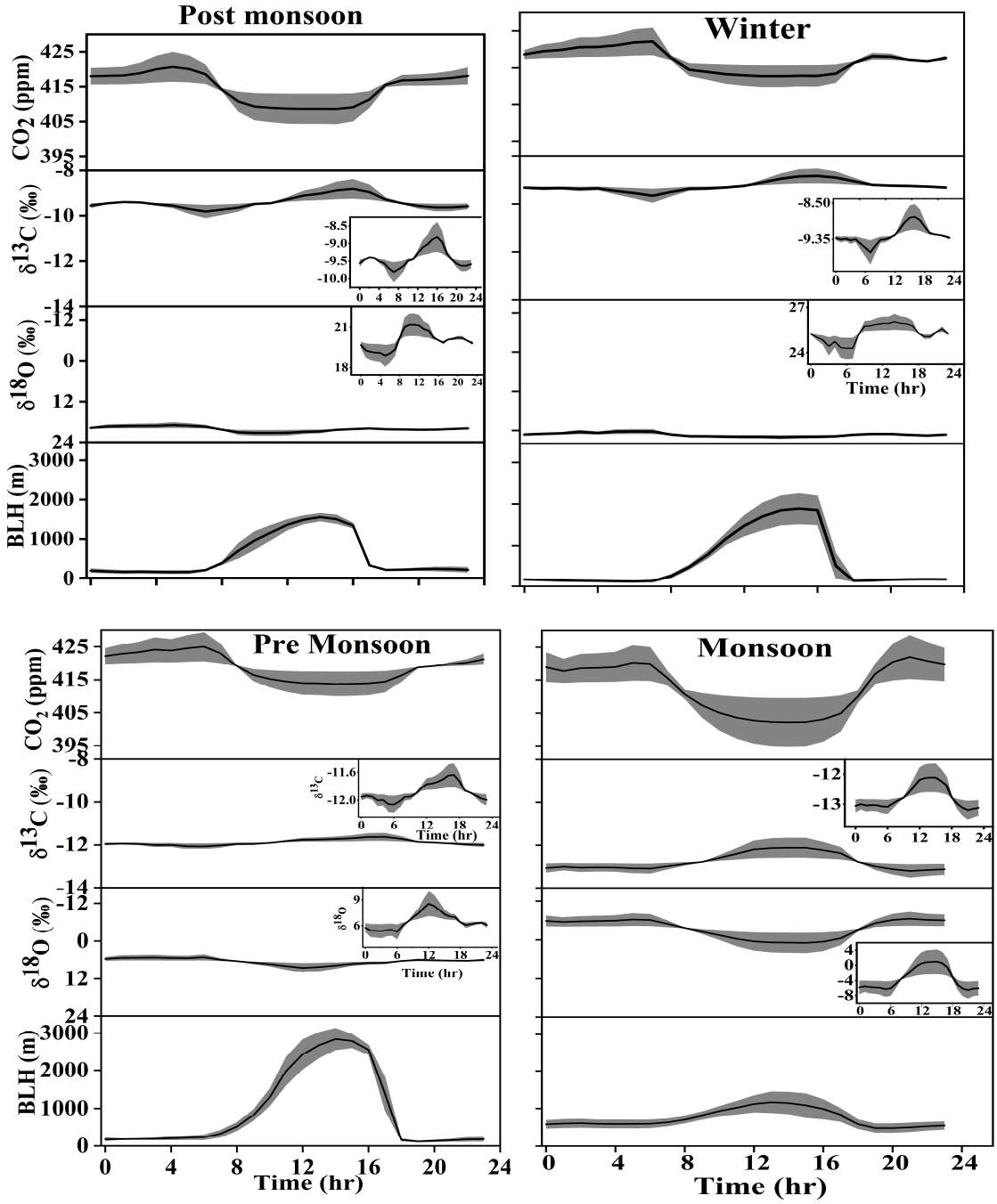

Figure 3. Diurnal variation of seasonally averaged CO_2, $\delta^{13}C$-CO_2, $\delta^{18}O$-CO_2 and boundary layer height during the study period. Grey shaded region represents the 1STD.

The monthly averaged with 1STD of atmospheric CO_2, $\delta^{13}C$-CO_2 and $\delta^{18}O$-CO_2 during the study period are shown in figure 2. At the study site, the annual averaged atmospheric CO_2 concentrations and ^{13}C-CO_2 and ^{18}O-CO_2 are 414.76±4.26 ppm, -11.19±1.63 ‰ and 9.02 ±12.78 ‰.

The study site experience 4 seasons namely post-monsoon (November-December, vegetation-II), winter (January-February), pre-monsoon (March-May, also known as summer months-dry season) and summer monsoon (June-September; vegetation-I). The NDVI in figure 1 show maximum during monsoon and minimum during rest of the seasons. Seasonal averages of CO_2 ($\delta^{13}C$-CO_2 & $\delta^{18}O$-CO_2) during post-monsoon, winter, pre-monsoon and summer monsoon are 414.70±4.49 ppm (-9.41±0.27 ‰ & 20.03±0.73 ‰), 416.84±3.25 ppm (-9.25±0.21 ‰, & 25.95±0.57 ‰), 418.88±4.07 ppm (-11.88±0.13 ‰ & 6.51±0.98 ‰), 412.61±7.59 ppm (-12.76±0.38 ‰ & -3.49±2.87 ‰) respectively. Site specific $\delta^{13}C$-CO_2 seasonal values with other study sites in India and across the world are summarized in table 2. Liu et al. (2014) showed annual means of $\delta^{13}C$-CO_2 varying from -8.30 ‰ to -8.35 ‰ at Waliguan station in China. Further, the annual means of $\delta^{13}C$-CO_2 are -8.27 ‰ and -8.36 ‰ respectively for 2009 and 2010 at Shangdianzi station which is located in a small village about 100 km northeast of Beijing (second populated urban city in China). This site is influenced by strong pollution events from Beijing and surrounding urban areas in the presence of southwesterly winds. Also, the annual mean of $\delta^{13}C$-CO_2 were -8.55‰, -8.52%, -8.46% and -8.61% during 2007-2010 at Tae-ahn Peninsula which is located on a small Peninsula on the western coast of Korea. Irrespective of the sites background influence, results of worldwide sites mentioned above indicates $\delta^{13}C$-CO_2 values are in close proximity with our present observations. An increase and decrease of $^{18}O/^{16}O$ ($\delta^{18}O$) ratio of CO_2 in the atmosphere across the seasons indicates dominance of photosynthesis and ecosystem respiration. During the study period, the atmospheric $\delta^{18}O$–CO_2 varies seasonally from -3.49‰ to + 25.95‰ with large scatter compared to seasonal CO_2 and $\delta^{13}C$. The scatter could be due to vegetation cover, leafwater content, retention of soil water and ocean (Zhou et al., 2006). However, interpretation of seasonal $\delta^{18}O$-CO_2 is not that straight as CO_2 and $\delta^{13}C$-CO_2 due to the varying fluxes of biospheric CO_2 and prevailing meteorology at the study site.

High atmospheric CO_2 in pre-monsoon followed by winter and subsequent increase of $\delta^{18}O$-CO_2 in the atmosphere in the absence of relatively low photosynthesis could be attributed to long-range air mass transport with enhanced $\delta^{18}O$-CO_2 (Murayama et al., 2010) and fossil fuel burning activities. Through isotopic exchange, $\delta^{18}O$-CO_2 in the atmosphere may affect due to variation in the ^{18}O from precipitation and soil respiration (Kato et al., 2004). The range of $\delta^{18}O$-CO_2 at Los Angeles basin, Southern California during 1972 -1973 (1998-2003) is -3.56 ‰ to + 0.21 ‰ (-3.99 ‰ to +0.45 ‰) and average value during 1972-1973 (1998-2003) of $\delta^{18}O$-CO_2 is -1.28 ‰ (-1.07‰) (Newman et al., 2008).

Thus, figure 3 shows diurnal variations of seasonally averaged CO_2, $\delta^{13}C$-CO_2 and $\delta^{18}O$-CO_2 against BLH. The height of the BL is the vertical extent of air column driven by convection processes associated with the earth's surface heating (Stull, 1988). Due to strong convection and associated surface temperature, the BLH attains maximum height in the afternoon, which modulates the dispersion of air pollutats in the mixed layer. In contrast to this, the BLH quickly dissipates and reaches stable form during night hours due to the absence of convection processes. Irrespective of seasons, diurnal variation of atmospheric CO_2 showed minimum (maximum) concentration against maximum (minimum) BLH between 12:00 IST to 16:00 IST (6:00 IST and 20:00 IST). The diurnal peak of the BLH is maximum (minimum) in pre-monsoon (summer monsoon) with 2839 m (1167 m) respectively, which indicates strong convection in the dry season. Subsequently, observed low (high) CO_2 concentration during strong (absence) convective hours. The observed diurnal cycle of CO_2 is closely associated with diurnal variation of the BLH. The maximum mean value of CO_2 is 418.88 ± 4.07 ppm in pre-monsoon during the study period. An afternoon drop of CO_2 during the study period is associated with the destructed

stable BLH and active photosynthetic process in daytime. In contrast, large variability in diurnal atmospheric CO_2 is observed during the summer monsoon with low BLH (1167 m). Thus, exhibits prominent diurnal variations of CO_2 and $\delta^{13}C$-CO_2 against BLH during all the seasons which is also attributed to isotopic fractionation processes during biological activity (Demény and Haszpra 2002). Except for monsoon, diminished diurnal seasonal variability observed with $\delta^{18}O$-CO_2 (Murayama et al., 2010) compared to CO_2 and $\delta^{13}C$-CO_2 at present site. Besides the influence of BLH, minimum CO_2 and maximum $\delta^{13}C$-CO_2 and $\delta^{18}O$-CO_2 during afternoon hours are due to the uptake of CO_2 by the plants through photosynthesis process. During night hours, the concentration CO_2 is maximum with low $\delta^{13}C$-CO_2 and $\delta^{18}O$-CO_2 due to active terrestrial respiration (Sreenivas et al., 2016). Therefore, diurnal patterns of CO_2 and $\delta^{13}C$-CO_2 are anti-correlated during all the seasons with minimum CO_2 in daytime and maximum $\delta^{13}C$-CO_2 respectively (figure 3). Similarly, Pang et al. (2016) observed a negative relationship of $\delta^{13}C$-CO_2 diurnal cycle with CO_2 mixing ratio at Beijing, in Northern China.

Study sites	**$\delta^{13}C$-CO_2 values (‰) Seasonal**	**References**
Dallas, USA	-12.0 to -8.1	Clark-Thorne and Yapp, 2003
Bern, Switzerland	-14 to -8	Sturm et al.,2006
Salt Lake City, USA	-18 to -8 (Dec 2004 - Jan 2005)	Pataki et al., 2006
Los Angeles, USA	-9.3 to -7.5 (Oct) -12.5 to -8.8 (Dec) -12.2 to -9.2 (Feb) -12.5 to -10.2 (April)	Djuricin et al., 2010
Nagoya, Japan	-13.4 to -8.5(May) -15.0 to -8.5 (Dec from 2008 - 2009)	Wada et al., 2011
Krakow, Poland	-11 to -9.5	Zimnoch et al., 2012
Wroclaw (SW Poland)	-16.4 to -8.2	Gorka et al., 2013
Cabo de Rama (West Coast of India)	-8.4 to -7.8	Bhattacharya et al., 2009
Bangalore, India	-9.31 to -8.04	Guha and Ghosh, 2015
NRSC, Shadnagar, India	-12.8 to -9.3 (Nov 2018 - Oct 2019)	Present study

Table 2. $\delta^{13}C$-CO_2 values from different study sites.

Seasonal variability of diurnal atmospheric CO_2 was 9.82 ±1.39 ppm, 7.19 ± 0.11 ppm, 9.23 ±2.1 ppm and 17.30 ±9.29 ppm in post-monsoon, winter, pre-monsoon and summer monsoon respectively during the study period (figure 3). Weak and strong seasonality was observed during winter and monsoon seasons repectively reflecting enrichment of atmospheric CO_2 in low vegetation months and depleting CO_2 in high vegetationseason. The diurnal variability of seasonal $\delta^{13}C$-CO_2 ($\delta^{18}O$-CO_2) are 0.48 ± 0.06 ‰ (1.91±0.005 ‰), 0.44 ±0.02 ‰ (1.60 ±0.13 ‰), 0.32 ± 0.09 ‰ (2.53 ±1.003 ‰) and 0.87 ± 0.73 ‰ (6.58 ± 4.10 ‰) in post-monsoon, winter, pre-monsoon and summer monsoon respectively. These amplitudes at our site are lower as compared to urban region listed in Table 2. The Sinhagad (located over the Western Ghats mountains) and Cape Rama, Goa (located close to the shoreline) of western India showed CO_2 seasonal amplitudes between 8-10 ppm during monsoon and >15ppm for remaining seasons (Tiwari et al., 2014), which could be due to the influence of monsoon circulation and strong local -regional biospheric activity (Metya et al., 2021). Thus, modulation in the seasonal amplitude of CO_2 in the atmosphere is attributed to the rate of photosynthesis and respiration besides the impact of local and long-range prevailing meteorology. For better understanding of the relationship between atmospheric CO_2 against its stable isotopic composition, improved model by Miller and Tans was adopted by fitting linear regression using the OLS.

3.2. Seasonal correlation between CO_2, and $\delta^{13}C$-CO_2 using the improved model by Miller and Tans

Since the study site is not a single sourced location and is closed proximity of Hyderabad, a metropolitan city of India, the Miller-Tans (2003) method was applied on the day and night time observations to characrterize the effective $\delta^{13}C$ ($^{13}C/^{12}C$) source ratios at the study site. In order to estimate the slope (δ_s) for $\delta^{13}C$-CO_2, the OLS curve fitting was applied to ΔCO_2 against $\Delta(CO_2 \times \delta^{13}C)$ and results shown in Figure 4. The modified Keeling method is applied to capture the processes of day and night which are driving the atmospheric CO_2. During the day (night) time $\delta^{13}C$-CO_2 slopes in post-monsoon, winter, pre-monsoon and monsoon are -10.43±5.60 ‰ (-27.08±4.21 ‰), -36.43±8.11 ‰ (-25.11±5.55 ‰), -32.02±4.57 ‰ (-23.79±2.08 ‰) and -52.50±4.60 ‰ (-27.30±0.36 ‰) respectively. During day and nighttime hours, the correlation coefficient ('r') was poor (-0.24 to -0.78) in postmonsoon, winter and premonsoon, which is small to estimate the source value. However, a strong 'r' value of -0.91 was found during the nighttime hours in monsoon season (Röckmann et al., 2016; Vardag et al., 2016), thus estimated the source signature (δ_s) using OLS (-27.30±0.36 ‰) and RMA (-37.42±0.73 ‰) methods. The $\delta^{13}C$ slope during daytime is largely varied in all the seasons representing the contribution of mixed source emissions at the regional scale and suppressed local sources (Xu et al., 2017). An average value of daytime δ_s of $\delta^{13}C$ during all seasons is -32.84 ‰ indicating the source of atmospheric CO_2 is related to gasoline and natural gas combustion in and around the study site (Clark-Thorne and Yapp, 2003). The estimated slopes are evaluated statistically and found significant (p-value < 0.05) with 95 % confidence interval during all the seasons. The $\delta^{13}C$ slopes in nighttime during all the seasons are between -25.11 ‰ to -27.39 ‰, with an average value of -26.72 ‰. In general, the average value of δ_s of $\delta^{13}C$-CO_2 is -26.20 ‰ for C_3 ecosystem respiration (Pataki et al., 2003). Thus, the present study also confirm the dominance of C_3 vegetation at the study site contributes to the emissions of atmospheric CO_2 mixing ratio during night time. The varied δ_s of $\delta^{13}C$-CO_2 in different study locations are attributed to the the local anthropogenic activities and terrestrial biospheric pathways.

Large variability in atmospheric $\delta^{18}O\text{-}CO_2$ (Yakir et al., 2011) was noticed during the study period. However, a strong correlation of $\delta^{18}O$ with 'r' value of -0.86 was observed (Figure not shown) in night hours of monsoon, which coincidence with the $\delta^{13}C$ during the same season, indicating the active role of biospheric –atmospheric interactions in the exchange of CO_2. With the present study, we understand that interpretation of the seasonal $\delta^{18}O$ variation is complicated compared to $\delta^{13}C$ and CO_2 mixing ratio. However, current knowledge on $\delta^{18}O$ seasonality can be improved with great understanding of varying fluxes of bisopheric CO_2 and role of prevailing meteorology at the study site. Since poor correlation between $\Delta CO_2$and $\Delta(CO_2\times\delta^{13}C)$ during day and nighthours in all seasons except nighthours in monsoon, we further implemented OLS and RMA methods only on monsoon data to estimate the source/sink signature (δ_s) of atmospheric CO_2. Figure 4 show improved Miller and Tans method applied on monsoon data during nighthours and fitted with the OLS and RMA linear regression. The deduced slopes from the OLS and RMA are -27.30±0.36 ‰ and -37.42±0.73 ‰ respectively indicating probable contribution from fossil fuel combustion and dominance of C_3 ecosystem respiration. While swapping the x and y axis in the Miller Tans plots, the slopes obtained from the OLS and RMA methods remain statistically same with 'r' value of -0.91. This further confirms the efficacy of RMA regression on the Miller Tans plot in identifying the source CO_2.

The δ_s of $\delta^{13}C$ analysis at the study site confirms the prominence of C_3 ecosystem activities viz. photosynthesis and respiration in the variability of atmospheric CO_2 during vegetative seasons. During dry seasons (winter and pre-monsoon), the δ_s values indicates the important role of local and long-range combustion processes that enrich atmospheric CO_2 at the study site. However, this information is pertained to the total source contributions and individual source apportionment was not carried out in this study.

Season	**Daytime ΔCO_2vs$\Delta(CO_2\times\delta^{13}C)$**		**Nighttime ΔCO_2vs$\Delta(CO_2\times\delta^{13}C)$**	
	'r'	Slope (‰)	'r'	Slope(‰)
Postmonsoon	-0.24	-10.43±5.60	-0.64	-27.08±4.21
Winter	-0.51	-36.43±8.11	-0.51	-25.11±5.55
Premonsoon	-0.61	-32.02±4.57	-0.78	-27.39±2.08
Monsoon	-0.75	-52.50±4.60	-0.91	-27.30±0.36 (-37.42±0.73)*
*indicates the slope calculated using RMA method for the nighttime data during monsoon				

Table 3. Seasonal correlation coefficient (r), and slope (δs) derived from the improved Miller and Tans method fitted with the OLS and RMA.

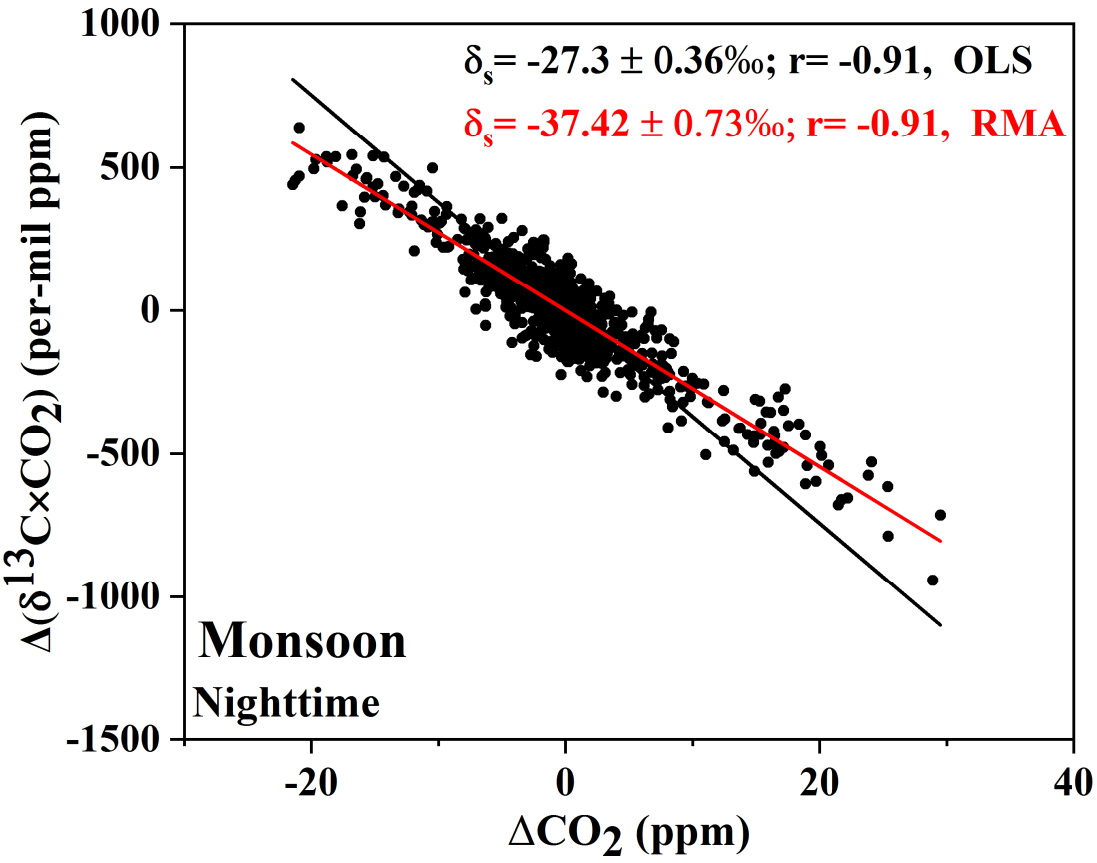

Figure 4. Improved Miller and Tans method applied to the monsoon seasonal ΔCO_2vs$\Delta(CO_2\times\delta^{13}C)$ during nighttime. The solid line black line and red coloar line represents the regression fit using ordinary least square method and reduced major axis method respectively.

Table 3 shows seasonal 'r' and slope values derived between ΔCO_2vs$\Delta(CO_2\times\delta^{13}C)$ and ΔCO_2vs$\Delta(CO_2\times\delta^{18}O)$during day and night hours respectively. During nighttime the average value of slope at the study site is close to C_3 ecosystem respiration and during daytime the average value of slope is close to sources which are combustion, photosynthesis processes and long range transport.The differences in slope value at various study sites is due to photosynthesis pathways and local anthropogenic sources prevailing at the study areas (Pang et al., 2016). In similar studies carried by various authors, reported slope values at their study site which is as follows. Liu et al. (2014) observed annual mean value of slope which is -25.44‰ and -21.70 ‰ at Waliguan and Shangdianzi stations in China respectively. Zhou et al. (2006) studied the isotopic fractionation at 11 stations of Northern Hemisphere and found slope (δ_s)ranging from -28.85‰ to -26.50‰ with improved Miller-Tans method. Murayama et al.(2010) observed δ_s value of -28.7‰ averaged over the study period at Takayama site in central Japan, which is also comparable to the present study site.

The correlation coefficient (r) between $\delta^{18}O$-CO_2 and $\delta^{13}C$-CO_2 during daytime (night time) are 0.13(0.07), 0.64(0.60), 0.95(0.93), 0.24(0.92) for post-monsoon, winter, pre-monsoon and summer monsoon seasons respectively. A very strong positive correlation (0.93 to 0.95) in day and night hoursduring pre-monsoon between $\delta^{18}O$-CO_2 and $\delta^{13}C$-CO_2 might be due to high vapour pressure deficit (VPD) than the post monsoon (low VPD). The high VPD and summer

conditions are supportive for high transpiration as well as photosynthetic activities as sunshine hours are more during pre-monsoon than post monsoon (approaching towards winter). Low δ^{13}C-CO_2 and δ^{18}O-CO_2 correlation during post-monsoon indicates high stomatal conductance in vegetation, ensuring enhanced release of water to the atmosphere (Cullen et al., 2008; Liu et al., 2014). Our study showed clear evidence of an increase or decrease of atmospheric CO_2 is associated with the changes of its isotopic composition during photosynthesis and biogenic respiration besides local and long-range anthropogenic influences. Also, Zimnoch et al. (2004) observed good correlation between δ^{18}O-CO_2 and δ^{13}C-CO_2 with 'r' ranging from 0.84 to 0.94 in their observations while studying their diurnal variability from Poland. Further to understand the influence of transport pathways on atmospheric CO_2 via long range airmass is examined in the present study using Hybrid Single Particle Lagrangian Integrated Trajectory Model (HYSPLIT) along with the forest fire count.

3.3. Influence of local and long-range airmass on atmospheric CO_2

Study site being a suburban region and about 60 km away from the Hyderabad city, the analysis of improved Miller-Tan model depicts atmospheric CO_2 concentration at the study site is mainly controlled by terrestrial biosphere activities during the study period. During the dayhours, the derived δ_s of δ^{13}C indicating mixed source contribution at the study site, which may be possibly due to combustion activities, biomass burning and the transportation of airmass. Seasonal wind vector obtained from the ECMWF at 850 hPa over the Indian region are shown in figure 5a. The long-range airmass circulation that is reaching the study site has been analyzed using Lagrangian back-trajectory model along with the firecounts during all the seasons (Figure 5b).

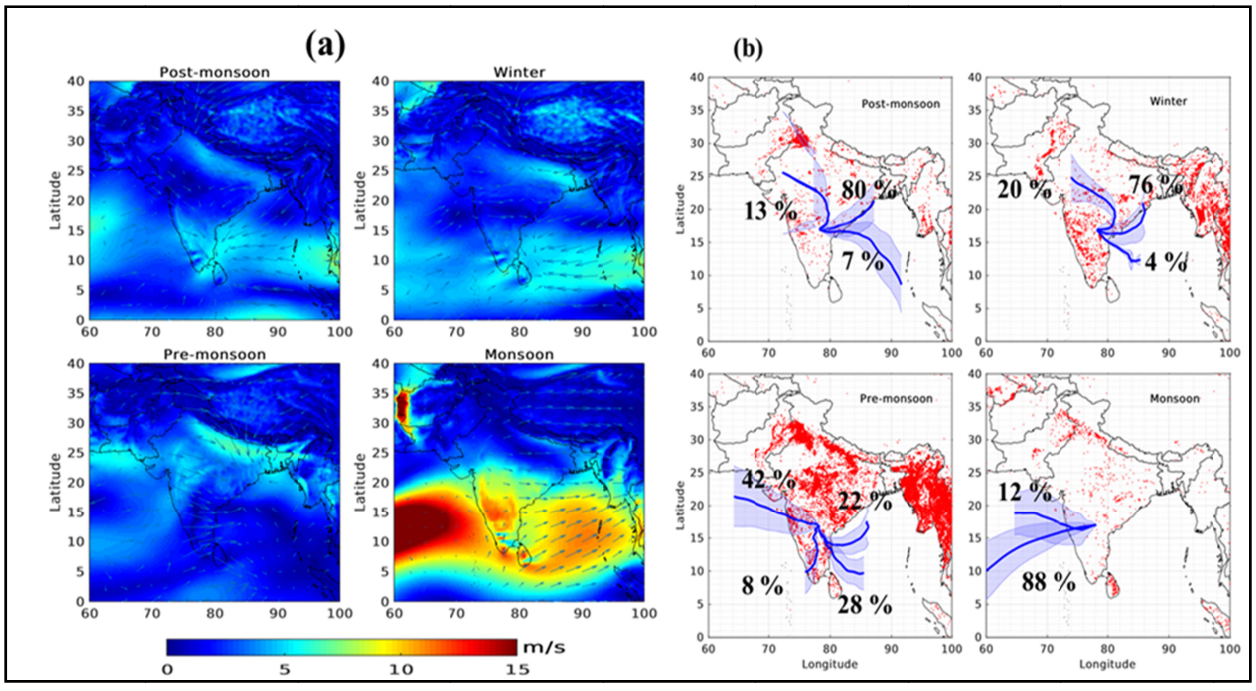

Figure 5 . (a) Mean winds (m s^{-1}) at 850 hPa (b) Seasonal long-range air mass circulation at 2 km altitude using HYSPLIT overlaid by forest fire count.

During the Indian summer-monsoon season, the south-westerly(SW) winds as shown in Figure 5a are in general dominate, which brings maritime airmass (Bhattacharya et al., 2009; Tiwari et al., 2014; Guha and Ghosh, 2015) over the Indian region.The atmospheric CO_2 concentration at the study site is observed minimum during the summer-monsoon period indicating the contribution of monsoon circulation through scavenging effect (Tiwari et al., 2014; Mahesh et al., 2014). The maritime airmass during summer-monsoon is relatively pristine due to the absence of anthropogenic sources thus observed low atmospheric CO_2 concentration at the study site.

A Lagrangian back trajectory analysis as shown in Figure 5b also confirms the observed low atmospheric CO_2 due to influence of maritime airmass (88 %) during the summer-monsoon period. During winter and pre-monsoon seasons, enrichment of atmospheric CO_2 at the study site could be due to the predominant continental sources reaching from the north-east (NE, 76 %) and north-west (NW, 42 %) respectively. Figure5b shows seasonal long-range air mass circulation over laid with fire count obtained from Moderate Resolution Imaging Spectroradiometer (MODIS) during the study period. During pre-monsoon and post-monsoon, agriculture residue burning is commonly observed in Punjab, Haryana and Indo Gangetic Plains (IGBP) areas of India (Liu et al., 2019), which are in NW and NE directions of the study site. Thus, the present study reveals that during these seasons, the biomass burning is one of continental sources contributing to the elevated CO_2 concentration.Therefore the variability of atmospheric CO_2 concentration at the study site is greatly influenced by the maritime airmass during summer-monsoon and continental sources during other seasons.

4. Conclusion

The present study examined the diurnal and seasonal variations of atmospheric CO_2 and its stable isotopes $\delta^{13}C$-CO_2 and $\delta^{18}O$-CO_2 at the sub-urban site of India during November 2018 to October 2019 using high precision CO_2 isotopic analyzer.
Following are the salient findings of the present study

1. The atmospheric CO_2 concentration ranged from 405 ppm to 450 ppm, with its stable isotopic composition ranging from -7.72 to -14.55 ‰ VPDB for $\delta^{13}C$ and from -24.63 to 28.91 ‰ VPDB for $\delta^{18}O$ respectively.
2. The CO_2 and $\delta^{13}C$-CO_2 exhibit clear diurnal variation with opposite patterns during all the seasons with minimum CO_2 and maximum $\delta^{13}C$-CO_2 in daytime and vice versa.
3. During strong convective hours (peak BLH) low atmospheric CO_2 concentration was observed. High CO_2 concentration was observed in weak convective period which indicates strong atmospheric mixing.
4. Diurnal variability of seasonal atmospheric CO_2 at the study site was 9.82 ± 1.39 ppm, 7.19 ± 0.11 ppm, 9.23 ±2.1 ppm and 17.30 ± 9.29 ppm in post-monsoon, winter, pre-monsoon and summer monsoon respectively. Large seasonality in summer-monsoon at the study site due to strong influence of monsoonal winds,precipitation and vegetation cover.
5. To capture the driving processes of atmospheric CO_2 during day and night hours, we thus applied improved Miller-Tans model on seasonal ΔCO_2, $\Delta(CO_2 \times \delta^{13}C)$ and $\Delta(CO_2$

615 ×$\delta^{18}O$) data. During all seasons, the nighttime δ_s values were between -25.11 ‰ to -
616 27.39 ‰, with an average value of -26.72 ‰ with moderate 'r' value.
617 6. However, a strong source/sink signature of $\delta^{13}C$ was observed during nighttime of
618 summer monsoon with the slope of -37.42±0.73 ‰, obtained using a reduced major axis
619 (RMA) regression. The source identified is attributed to combustion and dominance of
620 C_3 ecosystem respiration respectively.
621 7. Seasonal 'r' value between $\delta^{18}O$-CO_2 and $\delta^{13}C$-CO_2 during day and night time are varied
622 0.13 to 0.95 and 0.07 to 0.93 respectively. A very strong positive correlation (0.93 to
623 0.95) in day and night hours during pre-monsoon between $\delta^{18}O$-CO_2 and $\delta^{13}C$-CO_2
624 might be due to high VPD than the post monsoon (low VPD).
625 8. Upwind transport confirms the influence of biomass burning on enriched atmospheric
626 CO_2 during pre-monsson and post-monsoon seasons.
627 9. A lagrangian back-trajectories confirms the variability of atmospheric CO_2 concentration
628 at the study site is largely influenced by the maritime airmass during summer-monsoon
629 and continental sources in other seasons.
630
631 Our study showed clear evidence of an increase or decrease of atmospheric CO_2 is
632 associated with the changes of its isotopic composition during photosynthesis and
633 biogenic respiration besides local and long-range anthropogenic influences. The
634 variability in atmospheric CO_2 during monsoon season is strongly associated with the
635 ISM. However, the individual source apportionment of different sources is not discussed
636 in this present study.

637 ## Acknowledgements

638 Authors sincerely thank Dr Raj Kumar, Director NRSC for his kind encouragement and support
639 to carry out this work. This work was part of the Atmospheric CO_2 Retrievals and Monitoring
640 (ACRM) of the National Carbon Project (NCP) funded by CAP-IGBP. We greatly thank Dr. V.K
641 Dadhwal, Former Director, Indian Institute of Space Science and Technology, Trivandrum,
642 India and Project Director, NCP for reviewing the manuscript. Authors thank Dr. M.V.R
643 SeshaSai, Deputy Director, ECSA for his encouragement to carry this study. We greatly
644 acknowledge the HYSPLIT, ECMWF-ERA and MODIS fire teams for providing the scientific
645 data sets used in this study.
646
647
648 **Declaration of competing interest**
649 The authors declare no competing interests.
650
651
652 **Data Availabilty Statement**
653
654 The *in- situ* data may be available publicly once archival is completed.
655
656
657 ## References
658

Andres, R.J., Marland, G., Fung, I., & Matthews, E. (1996). A 1°× 1° distribution of carbon dioxide emissions from fossil fuel consumption and cement manufacture, 1950–1990. *Global Biogeochem Cycles*, 10(3), 419-429.https://doi.org/10.1029/96GB01523.

Baer, D. S., Paul, J. B., Gupta, M., & O'Keefe, A. (2002). In Diode Lasers and Applications in Atmospheric Sensing; Fried, A., Ed. In SPIE-The International Society for Optical Engineering: Bellingham, WA, Vol. 4817, pp. 167-176.

Ballantyne, A.P., Alden, C.B., Miller, J.B., Tans, P.P., & White, J.W.C. (2012). Increase in observed net carbon dioxide uptake by land and oceans during the past 50 years. *Nature*, 488, 70-72, doi:10.1038/nature11299.

Bhattacharya, S.K., Borole, D.V., Francey, R.J., Allison, C.E., Steele, L.P., Krummel, P., et al. (2009). Trace gases and CO_2 isotope records from Cabo de Rama, India. *Current Science* 97(9), 1336-1344.

Chakraborty S., Tiwari Y.K., Deb Burman P.K., Baidya Roy S., Valsala V. (2020) Observations and Modeling of GHG Concentrations and Fluxes Over India. In: Krishnan R., Sanjay J., Gnanaseelan C., Mujumdar M., Kulkarni A., Chakraborty S. (eds) Assessment of Climate Change over the Indian Region. Springer, Singapore. https://doi.org/10.1007/978-981-15-4327-2_4

Cullen, L. E., Adams, M. A., Anderson, M. J., & Grierson, P. F. (2008). Analyses of $\delta^{13}C$ and $\delta^{18}O$ in tree rings of Callitriscolumellaris provide evidence of a change in stomatal control of photosynthesis in response to regional changes in climate. Tree Physiology, 28(10), 1525-1533. doi: 10.1093/treephys/28.10.1525.

Djuricin, S., Pataki, D.E., &Xu, X. (2010). A comparison of tracer methods for quantifying CO_2 sources in an urban region. *Journal of Geophysical Research: Atomspheres* 115, 1–13, https://doi.org/10.1029/2009JD012236.

Demény A, Haszpra L (2002) Stable isotope compositions of CO_2 in background air and at polluted sites in Hungary. Rapid Commun Mass Spectrom 16:797–804

Farquhar, G. D., Lloyd, J., Taylor, J.A., Flanagan, L.B., Syvertsen, J. P., et al. (1993). Vegetation effects on the isotope composition of oxygen in atmospheric CO_2. *Nature*, 363(6428), 439-443,doi: 10.1038/365368b0

Francey, R. J., & Tans, P. P. (1987). Latitudinal variation in oxygen-18 of atmospheric CO_2. Nature, 327(6122), 495-497.

Górka, M., &Lewicka-Szczebak, D. (2013). One-year spatial and temporal monitoring of concentration and carbon isotopic composition of atmospheric CO_2 in a Wrocław (SW Poland) city area. *Applied geochemistry*, 35, 7-13. https://doi.org/10.1016/j.apgeochem.2013.05.010.

Guillon, S., Agrinier, P., &Pili, E., (2015). Monitoring CO_2 concentration and $\delta^{13}C$ in an underground cavity using a commercial isotope ratio infrared spectrometer. *Applied Physics B-Lasers and optics*, 119(1), 165-175. doi: 10.1007/s00340-015-6013-4.

Guha T, Ghosh P (2010) Diurnal variation of atmospheric CO_2 concentration and $\delta^{13}C$ in an urban atmosphere during winter—role of the Nocturnal Boundary Layer. *J AtmosChem* 65:1–12. doi:10.1007/s10874-010-9178-6.

Guha, T, and Ghosh P (2013) An experimental set-up for carbon isotopic analysis of atmospheric CO_2 and an example of ecosystem response during solar eclipse 2010. *Journal of Earth System Science* 122.3 (2013): 623-638.

Guha, T.and Ghosh, P. (2015). Diurnal and seasonal variation of mixing ratio and $\delta^{13}C$ of air CO_2 observed at an urban station Bangalore, India. Environmental Science and Pollution Research, 22(3), 1877-1890. https://doi.org/10.1007/s11356-014-3530-3.

Huang, J., Yu, H., Guan, X., Wang, G., &Guo, R., (2016). Accelerated dryland expansion under climate change, *Nature Climate Change*, 6, 166–171, http://dx.doi.org/10.1038/nclimate2837.

Kato, T., Nakazawa, T., Aoki, S., Sugawara, S., & Ishizawa, M. (2004). Seasonal variation of the oxygen isotopic ratio of atmospheric carbon dioxide in a temperate forest, Japan. *Global Biogeochem Cycles*, 18(2),https://doi.org/10.1029/2003GB002173.

Liu, L., Zhou, L., Vaughn, B., Miller, J. B., Brand, W. A., Rothe, M., & Xia, L. (2014). Background variations of atmospheric CO_2 and carbon-stable isotopes at Waliguan and Shangdianzi stations in China. *Journal of Geophysical Research: Atmospheres*, 119(9), 5602-5612.

Liu, X., An, W., Leavitt, S. W., Wang, W., Xu, G., Zeng, X., & Qin, D. 2014. Recent strengthening of correlations between tree-ring $\delta^{13}C$ and $\delta^{18}O$ in mesic western China: Implications to climatic reconstruction and physiological responses. Global and Planetary Change, 113, 23-33.http://dx.doi.org/10.1016/j.gloplacha.2013.12.005

Liu, T., Marlier, M. E., Karambelas, A., Jain, M., Singh, S., Singh, M. K., Gautam, R., &DeFries, R.S. (2019). Missing emissions from post-monsoon agricultural fires in northwestern India: regional limitations of MODIS burned area and active fire products.*Environmental Research Communications* 1(1), 011007,https://doi.org/10.1088/2515-7620/ab056c.

Machida, T., Kita, K., Kondo, Y., Blake, D., Kawakami, S., Inoue, G., & Ogawa, T. (2002). Vertical and meridional distributions of the atmospheric CO_2 mixing ratio between northern midlatitudes and southern subtropics. *Journal of Geophyical Research: Atmospheres* 107(D3), BIB 5-1-BIB 5-9,https://doi.org/10.1029/2001JD000910.

Mahesh, P., Sreenivas, G., Rao, P. V. N., Dadhwal, V. K., Sai Krishna, S. V. S., &Mallikarjun, K. (2015). High-precision surface-level CO_2 and CH_4 using off-axis integrated cavity output

spectroscopy (OA-ICOS) over Shadnagar, India.*International Journal of Remote Sensing* ,36(22), 5754-5765,https://doi.org/10.1080/01431161.2015.1104744.

Mahesh, P., Sreenivas, G., Rao, P. V. N., &Dadhwal, V. K. (2016). Atmospheric CO_2 retrieval from ground based FTIR spectrometer over Shadnagar, India.*Atmospheric Measurement Techniques Discussions,*https://doi.org/10.5194/amt-2016-177, 2016.

Mahalakshmi, D.V., Sujatha, P., Naidu , CV., and Chowdary, V.M. (2014). Contribution of vehicular emissions on urban air quality: results from public strike in Hyderabad.Indian Journal of Radio & Space Physics (IJRSP), 43(6), 340-348.

Metya, A., Datye, A., Chakraborty, S., Tiwari, Y. K., Sarma, D., Bora, A., and Gogoi, N. (2021). Diurnal and seasonal variability of CO_2 and CH_4 concentration in a semi-urban environment of western India. Scientific reports, 11(1), 1-13.

Miller JB and Tans PP (2003) Calculating isotopic fractionation from atmospheric measurements at various scales. Tellus Series B: Chemical and Physical Meteorology 55: 207–214.

Monastersky, R. (2013). Global carbon dioxide levels near worrisome milestone. *Nature*, 497 (7447), 13–14, https://doi.org/10.1038/497013a.

Murayama, S., C. Takamura, S. Yamamoto, N. Saigusa, S. Morimoto, H. Kondo, T. Nakazawa, S. Aoki, T. Usami, and M. Kondo (2010), Seasonal variations of atmospheric CO_2, $\delta^{13}C$, and $\delta^{18}O$ at a cool temperate deciduous forest in Japan: Influence of Asian monsoon, J. Geophys. Res., 115, D17304, doi:10.1029/2009JD013626.

Nalini, K., Sijikumar, S., Valsala, V., Tiwari, Y. K., & Ramachandran, R. (2019). Designing surface CO_2 monitoring network to constrain the Indian land fluxes. *Atmospheric Environment* 218(1), 117003, https://doi.org/10.1016/j.atmosenv.2019.117003

Newman, S., Xu, X., Affek, H. P., Stolper, E., & Epstein, S. (2008). Changes in mixing ratio and isotopic composition of CO_2 in urban air from the Los Angeles basin, California, between 1972 and 2003. *Journal of Geophysical Research: Atmospheres*, 113(D23).https://doi.org/10.1029/2008JD009999

Pang, J., Wen, X., & Sun, X. (2016). Mixing ratio and carbon isotopic composition investigation of atmospheric CO_2 in Beijing, China. *Science of Total Environment* 539, 322-330,DOI: 10.1016/j.scitotenv.2015.08.130.

Pataki, D. E., Ehleringer, J. R., Flanagan, L. B., Yakir, D., Bowling, D. R., Still, C. J., ... & Berry, J. A. (2003). The application and interpretation of Keeling plots in terrestrial carbon cycle research. Global biogeochemical cycles, 17(1).

Pataki, D.E., Bowling, D.R., Ehleringer, J.R., & Zobitz, J.M. (2006). High resolution atmospheric monitoring of urban carbon dioxide sources. *Geophysical Research Letters* 33, 1–5,https://doi.org/10.1029/2005GL024822.

Röckmann, T., Eyer, S., Veen, C. van der, Popa, M.E., Tuzson, B., Monteil, G., Houweling, S., Harris, E., Brunner, D., Fischer, H., Zazzeri, G., Lowry, D., Nisbet, E.G., Brand, W.A., Necki, J.M., Emmenegger, L., Mohn, J. (2016). In situ observations of the isotopic composition of methane at the Cabauw tall tower site. Atmospheric chemistry and physics, 16(16), 10469-10487.https://doi.org/10.5194/acp-16-10469-2016.

Sharma, N., Dadhwal, V. K., Kant, Y., Mahesh, P., Mallikarjun, K., Gadavi, H., Sharma, A., & Ali, M. M. (2014). Atmospheric CO_2 variations in two contrasting environmental sites over India. *Air soil and water Research*, 7, ASWR-S13987,https://doi.org/10.4137/ASWR.S13987.

Smith, H. J., Fischer, H., Wahlen, M., Mastroianni, D., & Deck, B. (1999). Dual modes of the carbon cycle since the Last Glacial Maximum. *Nature*, 400(6741), 248-250.

Sreenivas, G., Mahesh, P., Subin, J., Kanchana, A. L., Rao, P. V. N., &Dadhwal, V. K. (2016). Influence of meteorology and interrelationship with greenhouse gases (CO_2 and CH_4) at a suburban site of India. *Atmospheric Chemistry and Physics* 16, 3953-3967,doi.org/10.5194/acp-16-3953-2016, 2016.

Sturm, P., Leuenberger, M., Valentino, F.L., Lehmann, B., &Ihly, B. (2006). Measurements of CO_2, its stable isotopes, O_2/N_2, and Rn-222 at Bern, Switzerland. *Atmospheric Chemistry and Physics*. 6, 1991-2004,https://doi.org/10.5194/acp-6-1991-2006, 2006.

Thorne, S. T., & Yapp, C. J. (2003). Stable carbon isotope constraints on mixing and mass balance of CO_2 in an urban atmosphere: Dallas metropolitan area, Texas, USA. *Applied Geochemistry*, 18(1), 75-95,https://doi.org/10.1016/S0883-2927(02)00054-9.

Thoning, K. W., Tans, P. P., &Komhyr, W. D. (1989). Atmospheric carbon dioxide at Mauna Loa Observatory: 2. Analysis of the NOAA GMCC data, 1974–1985. Journal of Geophysical Research: Atmospheres, 94(D6), 8549-8565.

Tiwari, Y. K., Vellore, R. K., Kumar, K. R., van der Schoot, M., & Cho, C. H. (2014). Influence of monsoons on atmospheric CO_2 spatial variability and ground-based monitoring over India. *Science of The Total Environment*, 490, 570-578, https://doi.org/10.1016/j.scitotenv.2014.05.045

Valsala, V., Tiwari, Y. K., Pillai, P., Roxy, M., Maksyutov, S., &Murtugudde, R. (2013). Intraseasonal variability of terrestrial biospheric CO_2 fluxes over India during summer monsoons. *Journal of Geophysical Research-Biogeosciences*, 118(2), 752-769, https://doi.org/10.1002/jgrg.20037.

Vardag, S. N., Hammer, S., & Levin, I. (2016). Evaluation of 4 years of continuous $\delta^{13}C$ (CO_2) data using a moving Keeling plot method. Biogeosciences, 13(14), 4237-4251.https://doi.org/10.5194/bg-13-4237-2016.

Wada, R., Pearce, J.K., Nakayama, T., Matsumi, Y., Hiyama, T., Inoue, G., & Shibata, T.(2011). Observation of carbon and oxygen isotopic compositions of CO_2 at an urban site in

Nagoya using mid-IR laser absorption spectroscopy. *Atmospheric Environment*, 45, 1168–1174,https://doi.org/10.1016/j.atmosenv.2010.10.015.

Xu, W., Ruhl, M., Jenkyns, H.C., Hesselbo, S.P., Riding, J.B., et al. (2017). Carbon sequestration in an expanded lake system during the Toarcian oceanic anoxic event. *Nature Geoscience*, 10, 129-134, doi: 10.1038/NGEO2871

Yakir, D. (2011). The paper trail of the ^{13}C of atmospheric CO_2 since the industrial revolution period. *Environmental Research Letters* 6(3), 034007,http://dx.doi.org/10.1088/1748-9326/6/3/034007.

Zhou, L., Conway, T. J., White, J. W., Mukai, H., Zhang, X., Wen, Y., Li, Jinlon.,&MacClune, K. (2005). Long-term record of atmospheric CO_2 and stable isotopic ratios at Waliguan Observatory: Background features and possible drivers, 1991–2002. *Global Biogeochemical Cycles,* 19(3), https://doi.org/10.1029/2004GB002430.

Zhou, L., J. W. C. White, T. J. Conway, H. Mukai, K. MacClune, X. Zhang, Y. Wen, and J. Li (2006), Long-term record ofatmospheric CO_2 and stable isotopic ratios at Waliguan Observatory: Seasonally averaged 1991–2002 source/sink signals, and acomparison of 1998–2002 record to the 11 selected sites in the Northern Hemisphere, Global Biogeochem. Cycles, 20, GB2001,doi:10.1029/2004GB002431.

Zimnoch, M., Florkowski, T., Necki, J. M., &Neubert, R. E. (2004). Diurnal variability of $\delta^{13}C$ and $\delta^{18}O$ of atmospheric CO_2 in the urban atmosphere of Kraków, Poland. Isotopes in Environmental and Health Studies, 40, 129-143. https://doi.org/10.1080/10256010410001670989.